Dual High-Selectivity Band-Notched Ultra-Wideband Filter with Improved Out-of-Band Rejection

Ying Jiang Guo [1], Xiao Hong Tang [1], and Kai Da Xu [2,3]

[1] EHF Key Lab of Science, University of Electronic Science and Technology of China, Chengdu, 611731, China

[2] Department of Electronic Science, Xiamen University, Xiamen, 361005, China

[3] Shenzhen Research Institute of Xiamen University, Shenzhen 518057, China
kaidaxu@xmu.edu.cn

Abstract ─ A novel microstrip ultra-wideband (UWB) filter with dual notched bands is presented. By placing a simple dual-mode resonator having two symmetrical outer high-impedance lines beside the UWB filter, two controllable rejection bands are created, each of which features two resonant modes and high frequency selectivity. Defected ground structure techniques (DGS) is applied to realize wide out-of-band attenuation. To explain band-notched operating mechanism, the parametric studies and equivalent circuit of the proposed structure are presented. The experimental results agree well with the predicted results declaring the advantages of the proposed structure with high-selectivity wide-bandwidth notched bands and improved out-of-band rejection.

Index Terms ─ Band-notched filter, high frequency selectivity, improved out-of-band rejection, ultra-wideband filter.

I. INTRODUCTION

Research on design and development of ultra-wideband (UWB) bandpass filters (BPF) have attracted great attention as the release of unlicensed UWB spectrum (3.1–10.6 GHz) by the Federal Communications Commission (FCC) for hand held devices in indoor environment [1]. There have existed various structures for UWB generation [2-14]. One common method for the design of an UWB-BPF is the use of multiple-mode resonators (MMRs), which possesses the flexibility of placing resonant modes at frequencies of interest in the passband [2-5]. Other methods were also presented to achieve UWB response, such as back-to-back broadside coupled structure [6], cascading lowpass and highpass filter [7], etc. However, many critical issues still puzzle researchers. One such challenge is to eliminate the frequency interference between UWB system and other wireless systems which have already occupied some operating bands of UWB system, especially like IEEE 802.11a (5.15 ~ 5.35 GHz & 5.725 ~ 5.825 GHz) and X-band military radar. Moreover, to achieve higher data rates, many systems including LTE Carrier Aggregation manage to increase their spectrum bandwidths, which, in turn, requires wider rejection band for the UWB design. Therefore, it is significantly necessary to introduce more than one wide-bandwidth notched-band responses into UWB filters.

Several methods to introduce notched bands in UWB filters were reported, such as etching slots on the ground [8], [9], embedding spurlines or stubs on the transmission line [10-12], and loading a resonator beside the original structure [13-15]. However, most structures in these filters can only generate one notched frequency band, which means that more complex structures are required when it comes to multiple notched bands, i.e., more than one resonators/stubs, MMRs, etc. Although some MMRs have been adopted for more than one band-notched generation [16-18], they show narrow rejection bandwidth and unsatisfactory frequency selectivity.

In this paper, by using only one simple dual-mode resonator and two high-impedance lines, a novel dual wideband band-notched UWB filter has been realized. With the help of two symmetrical outer high-impedance lines beside the microstrip feed line, the proposed resonators can produce two stopbands with higher rejection level and better frequency selectivity than that of only one stopband using the same resonator without outer lines. Moreover, the dumbbell-shape DGS helps to realize wide out-of-band rejection band. In Section II, the proposed resonator and its design evolution are demonstrated. Comparison between the proposed resonator and the conventional ones is made, showing clearly the advantage of the proposed structure. Parametric analysis and mathematical explanation provide guidelines to facilitate design process. In Section III, a UWB filter is designed and then the proposed resonator is loaded on this UWB filter for dual high-selectivity notched bands generation. Finally, a short

Submitted On: April 9, 2016
Accepted On: July 12, 2016

conclusion is given in Section IV.

II. BAND-NOTCHED RESONATOR ANALYSIS

The conventional resonator and modified structure as shown in Fig. 1 are used to evoke notched bands for the UWB filters. The conventional resonator is a folded half-wavelength resonator with a grounding via in the center, while the modified structure is developed with two additional symmetrical high-impedance outer lines connecting the conventional resonator to feed line. For size reduction, the outer lines are meandered. Figure 1 (c) illustrates the corresponding circuit model of Fig. 1 (b). The outer high-impedance lines can be equivalent to a series inductor-capacitor tank (L_2 and C_2), and the broad side coupling between two open stubs in Fig. 1 (b) is modeled as a capacitor C_1. Additionally, the via hole acts as an inductor L_1. The physical dimensions of the proposed resonator can be determined by using this model.

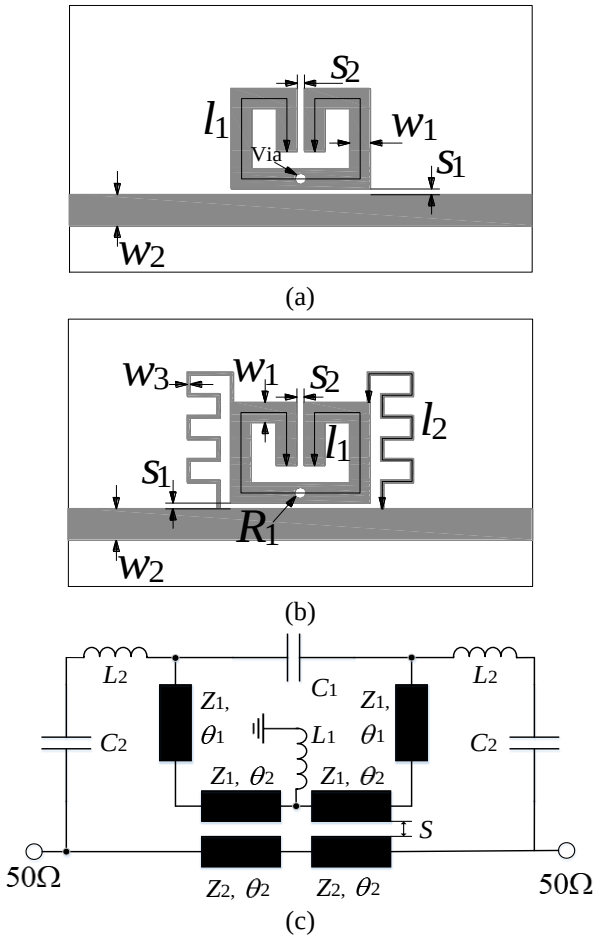

Fig. 1. (a) Layout of the conventional resonator, (b) the proposed structure, and (c) corresponding circuit model.

To analyze the characteristics of this proposed resonator, the resonators depicted in Fig. 1 are modeled with the help of full-wave electromagnetic simulation. All the structures in this paper are designed on a RT/Duorid 4350 substrate with a dielectric constant 3.48, thickness of 0.508 mm, and dielectric loss tangent value of 0.004. Figure 2 shows the simulated S_{21} and S_{11} magnitudes of the three resonators types under weak coupling which have the same physical dimensions. Dual-resonance characteristics are obtained for Fig. 1 (a), while the one without via has only one resonant mode. This feature can be applied to create a wideband notched band. The resonant frequency of the conventional resonator f_r can be approximately calculated by:

$$f_r = \frac{c}{\lambda_g \sqrt{\varepsilon_{eff}}} \approx \frac{c}{2l_1 \sqrt{(\varepsilon_r + 1)/2}}, \quad (1)$$

where λ_g denotes the guided wavelength, c is the velocity of light in free space, and ε_{eff} denotes the effective dielectric constant of the substrate. Once two symmetrical outer high-impedance lines are added as shown in Fig. 1 (b), the center frequency of one notched band is almost the same with that of Fig. 1 (a), and interestingly an extra stopband is generated. Compared to the conventional resonator, both of these two notched bands exhibit higher rejection level and satisfactory frequency selectivity. Additionally, multiple reflection zeros are located at each side of the stopbands enhancing the passband impedance matching.

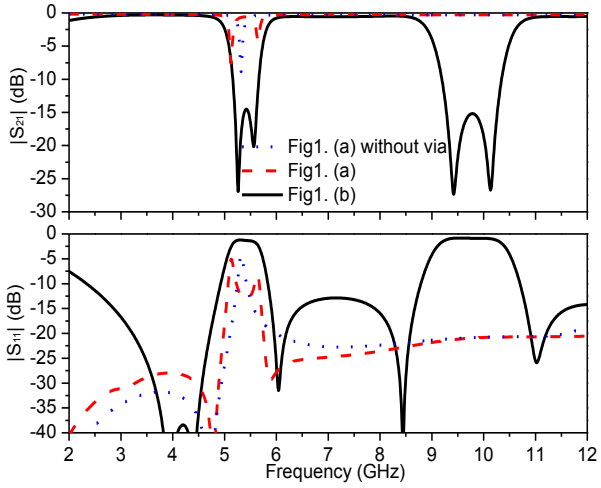

Fig. 2. Simulated results of the three resonators types (l_1 = 16.4, l_2 = 12.2, w_1 = 0.7, w_2 = 1.1, w_3 = 0.1, S_1 = 0.3, S_2 = 0.2, and the radius of via R_1=0.2, all in mm).

The center frequency of the extra stopband f_{r2} is primarily determined by the outer high-impedance lines equivalent to a series L_2-C_2 tank, which is approximately

calculated by:

$$f_{r2} \approx \frac{1}{2\pi\sqrt{L_2 C_2}}. \quad (2)$$

Here, L_2 and C_2 in this case equals to 3.48 nH and 0.08 pF, respectively, and the corresponding calculated f_{r2} is around 9.6 GHz, where the value is in order to make good agreement with the simulated center frequency of the higher stopband shown in Fig. 2. Due to the inductance much more than capacitance of the high-impedance lines equivalent circuit, adjusting the inductance L_2 is observed as shown in Fig. 3. When L_2 increases from 3.28 to 3.68 nH, the resonant frequency for the higher stopband will decrease gradually but the lower stopband almost keeps fixed.

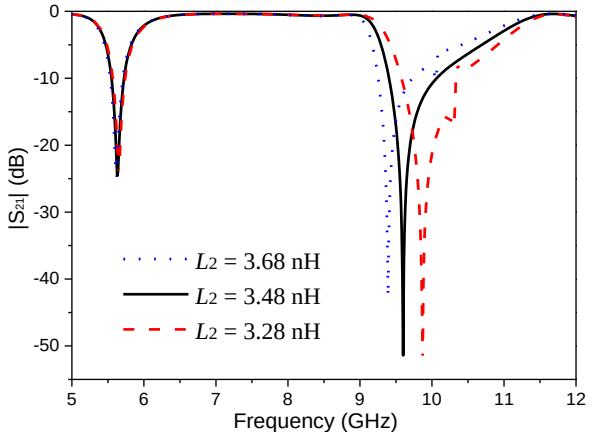

Fig. 3. Simulated $|S_{21}|$ variations with different L_2.

Furthermore, as the three important physical parameters (l_1, S_1, and S_2) have significant influence on the proposed resonator's frequency response, the proposed resonator having the same dimensions with discussed above are modeled and studied. Figure 4 demonstrates the predicted magnitude of S_{21} against frequency with different l_1, S_1, and S_2. As observed in Fig. 4 (a), the center frequencies of two stopbands both increase as l_1 changes from 16.9 to 15.9 mm, showing the length of the folded half-wavelength resonator l_1 affects both two stopbands. Obviously, l_1 is mainly determined by Equation (1) when the substrate material is chosen. When the gap between the resonator and feed line S_1 varies from 0.2 to 1.2 mm as seen in Fig. 4 (b), the center frequencies of the higher stopband experience an obvious drop, while the lower-frequency stopband changes slightly. Thus, the center frequencies of the two stopbands can be designed by tuning l_1, l_2, and S_1. In addition, the coupling gap S_2 can be used to adjust the bandwidth of the two stopbands (see Fig. 4 (c)). These graphs can be applied to simplify the proposed resonator design.

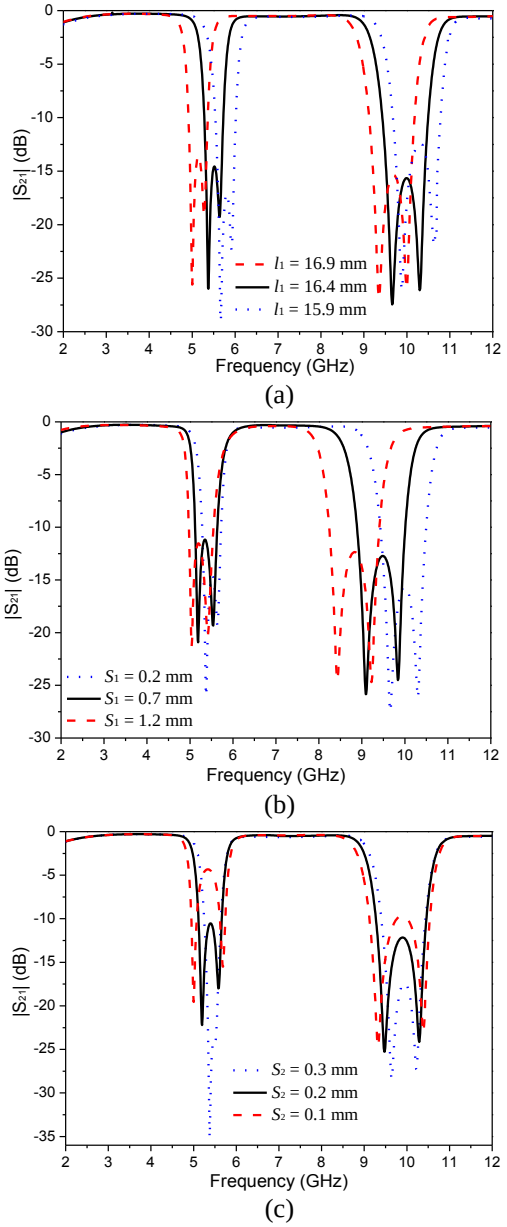

Fig. 4. Simulated $|S_{21}|$ variations with different: (a) l_1, (b) S_1, and (c) S_2.

III. DESIGN OF UWB FILTER WITH NOTCHED BANDS

A. UWB filter

Figure 5 depicts the layout and physical dimensions of the proposed basic UWB filter. The UWB response is developed based on the MMR which consists of a stepped-impedance resonator (SIR) loaded with one short-circuited stub and two symmetrical open-circuited folded stubs. Two interdigital coupled line sections are directly coupled to the two sides of the SIR. On the bottom layer of the filter, two tapered dumbbell-shaped

DGS units are designed to suppress the harmonic passband, since they can produce the transmission zeroes in the high frequency out-of-band range [19].

The frequency characteristics of the proposed MMR is presented in Fig. 6. Compared with previous MMR without DGS, open- and short-circuited stub, the proposed MMR can produce more resonant modes in UWB band improving the in-band impedance matching, and higher skirt selectivity is also achieved because the transmission zeros can be positioned close to the edge of UWB band.

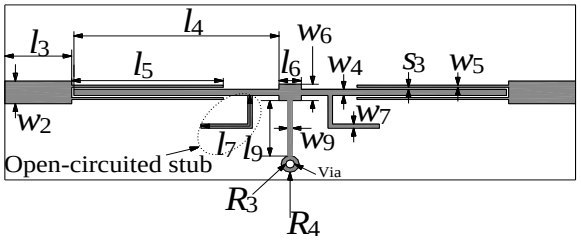

(a)

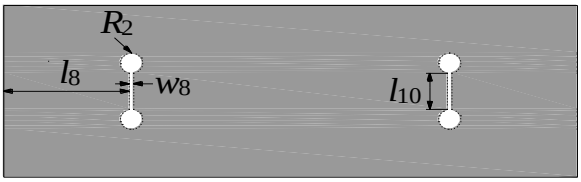

(b)

Fig. 5. Configuration of the basic UWB filter: (a) top layer and (b) bottom layer (w_2 = 1.1, w_4 = 0.3, w_5 = 0.1, w_7 = 0.2, w_8 = 0.2, w_9 =0.2, l_3 = 3, l_4 = 9.2, l_5 = 6.8, l_6 = 1, l_7 = 3.7, l_8 = 5.6, l_9 = 2.7, l_{10} = 1.8, w_6 = 0.8, R_1=0.2, and R_2 = 0.5, all in mm).

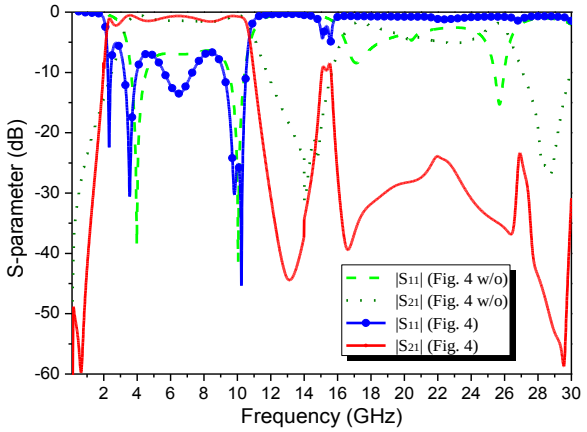

Fig. 6. Comparison between the basic UWB filter (Fig. 4) and its corresponding structure w/o (w/o: without DGS, open- and short-circuited stubs).

Figure 7 shows the simulated S_{21}-magnitudes of the proposed UWB structure under tight coupling case (interdigital coupled lines, S_3 = 0.1 mm) and weak coupling case (one coupled line, S_3 = 0.3 mm), respectively, where the other physical dimensions are the same. Four resonant modes are evoked in UWB band due to the proposed structure. Moreover, four resonant modes all increase as l_4 decreases, showing they are all affected by the length of the high-impedance line of SIR (see Fig. 8 (a)). Interestingly, only the first resonant mode are sensitive to l_9 (see Fig. 8 (b)), while as l_7 drops only the third and fourth resonant frequencies increase (see Fig. 8 (c)). It means that lengths of the short- and open-circuited stubs (i.e., l_9 and l_7) can be used to independently adjust the low- and high-frequency edge of the UWB band, respectively. Therefore, by carefully tuning the physical dimensions of the proposed resonator, the four resonant modes can be allocated properly to create the UWB response.

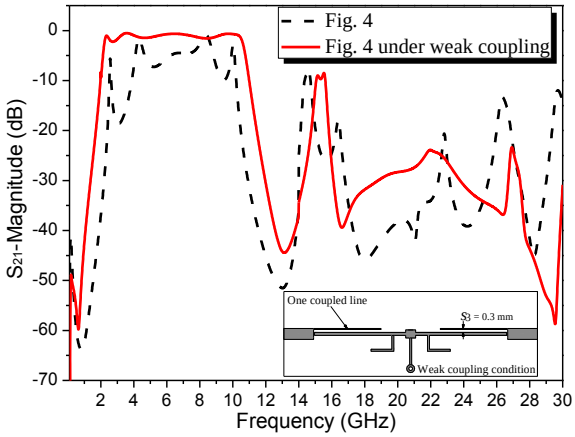

Fig. 7. Simulated S_{21}-magnitudes of the basic UWB filter and the same structure under weak coupling.

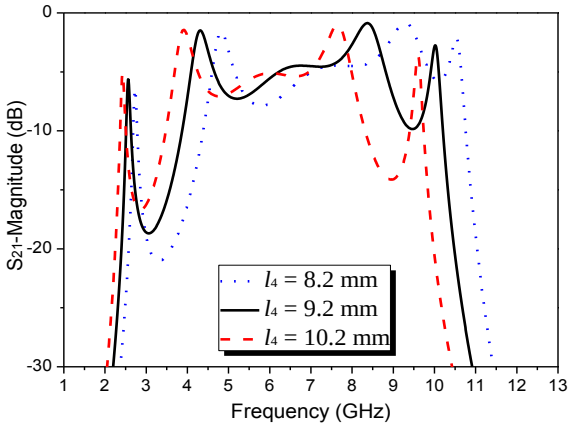

(a)

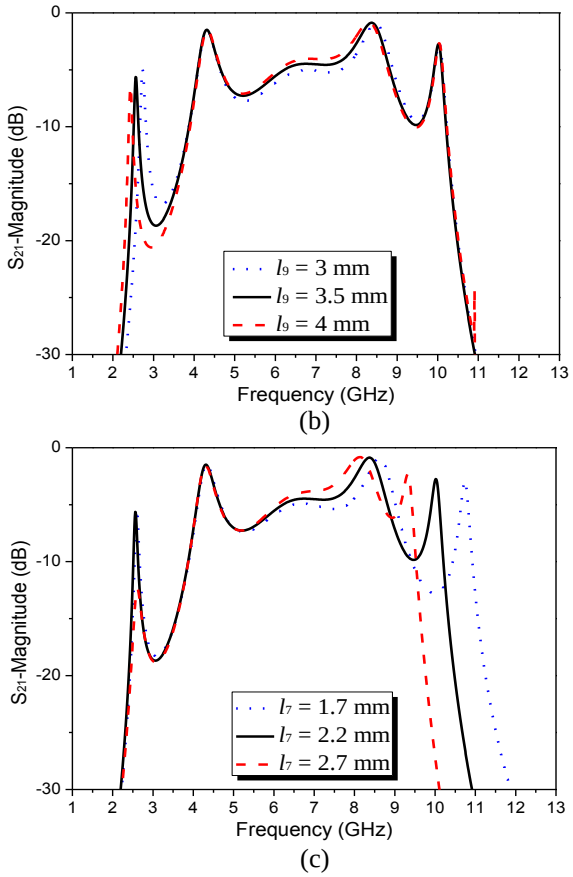

Fig. 8. Simulated S_{21} variations of the proposed MMR structure under weak coupling case with: (a) l_4, (b) l_9, and (c) l_7.

B. UWB filter loaded with the proposed resonator

In order to obtain notched band UWB response, the proposed band-notched resonator is added to the proposed basic UWB filter, as depicted in Fig. 9. The physical parameters of the loading notch resonator and basic UWB filter are assumed the same with those mentioned above. The whole structure is fabricated and its photograph is displayed in Fig. 10.

Figure 11 illustrates the simulated and measured S_{21}- and S_{11}-magnitudes as well as the group delays for the proposed band-notched UWB filter. They are found in good agreement with each other. The 3-dB passband covers the range of approximately 2.5–10.8 GHz (relative bandwidth: 124.8%) with the in-band measured insertion loss less than 2 dB except for the dual notched band (3-dB bandwidth: 4.95-5.85 GHz and 8.81-10.05 GHz). Each notched band has two resonant modes achieving wider bandwidth, while high frequency selectivity is also realized due to the intrinsic features of the proposed resonator. The measured upper-stopband is dramatically extended up to 30 GHz with an insertion loss larger than 20 dB due to the introduction of the out-of-band zeros caused by DGS units. In addition, the group delay varies between 0.2–1.4 ns within the UWB passband showing a good linearity, and significant drops are observed in the two stopbands.

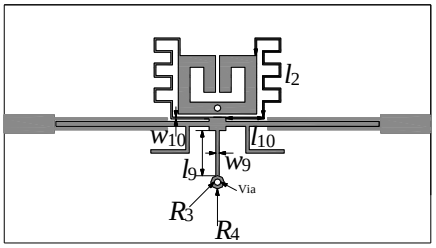

Fig. 9. Configuration of the proposed notched-band UWB filter.

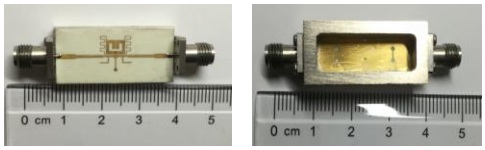

Fig. 10. Photograph of the fabricated dual band-notched UWB filter: (a) top view and (b) bottom view.

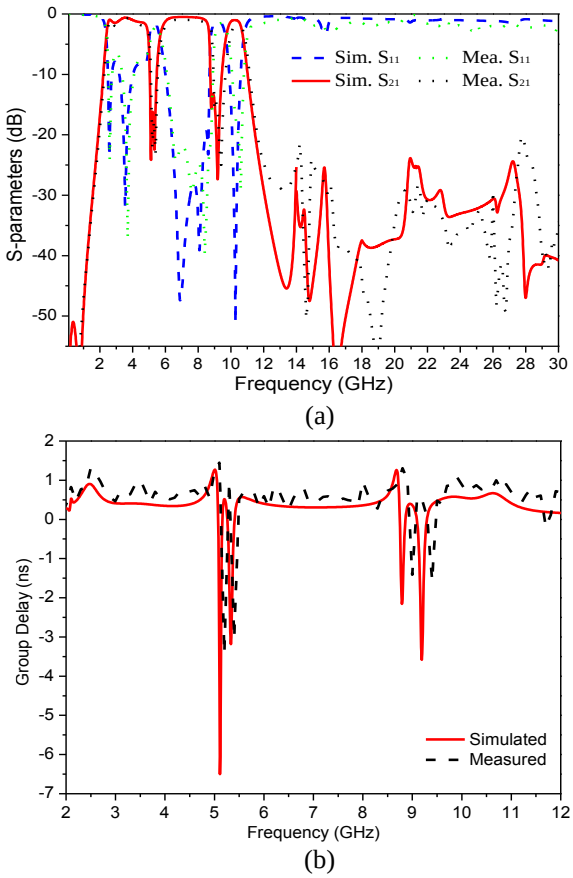

Fig. 11. Simulated and measured results of the proposed filter: (a) S-parameters and (b) group delays.

IV. CONCLUSION

To obtain dual notched bands with high frequency selectivity and wide bandwidth, a simple resonator with two symmetrical outer high-impedance lines connecting to the basic UWB filter has been proposed. Wide out-of-band attenuation is achieved by adopting DGS. Due to its simple structure and excellent performance, the proposed filters are expected to be good candidates for use in various UWB systems.

ACKNOWLEDGMENT

This work was supported in part by the Natural Science Foundation of Fujian Province of China (No. 2016J05164), and Guangdong Natural Science Foundation (No. 2016A030310375).

REFERENCES

[1] Federal Communications Commission, "First report and order in the matter of revision of part 15 of the Commission's Rules Regarding Ultra-Wideband Transmission Systems," ET-Docket 98-153, Apr. 22, 2002.

[2] L. Zhu, S. Sun, and W. Menzel, "Ultra-wideband (UWB) bandpass filters using multiple-mode resonator," *IEEE Microwave Wireless Comp. Lett.*, vol. 15, no. 11, pp. 796-798, 2005.

[3] R. Li and L. Zhu, "Compact UWB bandpass filter using stub-loaded multiple-mode resonator," *IEEE Microwave Wireless Comp. Lett.*, vol. 7, no. 1, pp. 40-42, 2007.

[4] Z. Zhang and F. Xiao, "An UWB bandpass filter based on a novel type of multi-mode resonator," *IEEE Microwave Wireless Comp. Lett*., vol. 22, no. 10, pp. 506-508, 2012.

[5] K. D. Xu, Y. H. Zhang, J. L. Li, W. T. Joines, and Q. H. Liu, "Compact ultra-wideband bandpass filter using quad-T-stub-loaded ring structure," *Microwave Opt. Technol. Lett.*, vol. 56, no. 9, pp. 1988-1991, 2014.

[6] H. Wang and L. Zhu, "Ultra-wideband bandpass filter using back-to-back microstrip-to-CPW transition structure," *Electron. Lett.*, vol. 41, no. 24, pp. 1337-1338, 2005.

[7] C. W. Tang and M.-G. Chen, "A microstrip ultra-wideband bandpass filter with cascaded broadband bandpass and bandstop filters," *IEEE Trans. Microwave Theory Tech.*, vol. 55, no. 11, pp. 2412-2418, 2007.

[8] J. Q. Huang, Q. X. Chu, and C. Y. Liu, "Compact UWB filter based on surface-coupled structure with dual notched bands," *Progress in Electromagnetics Research*, vol. 106, pp. 311-319, 2010.

[9] S. G. Mao, Y. Z. Chueh, C. H. Chen, and M. C. Hsieh, "Compact ultra-wideband conductor-backed coplanar waveguide bandpass filter with a dual band-notched response," *IEEE Microwave Wireless Comp. Lett*., vol. 19, no. 3, pp. 149-151, 2009.

[10] F. Wei, L. Chen, Q. Y. Wu, X. W. Shi, and C. J. Gao, "Compact UWB bandpass filter with narrow notch-band and wide stop-band," *Journal of Electromagnetic Waves & Applications*, vol. 24, no. 7 pp. 911-920, 2010.

[11] C.-Y. Liu, T. Jiang, and Y.-S. Li, "A novel UWB filter with notch-band characteristic using radial-UIR/SIR loaded stub resonators," *Journal of Electromagnetic Waves & Applications*, vol. 25, no. 2, pp. 233-245 2011.

[12] Y. H. Chun, H. Shaman, and J. S. Hong, "Switchable embedded notch structure for UWB bandpass filter," *IEEE Microwave Wireless Comp. Lett*., vol. 18.no. 9, pp. 590-592, 2008.

[13] R. Ghatak, P. Sarkar, R. K. Mishra, and D. R. Poddar, "A compact UWB bandpass filter with embedded SIR as band notch structure," *IEEE Microwave Wireless Comp. Lett*., vol. 21, no. 5, pp. 261-263, 2011.

[14] J. Xu, W. Wu, W. Kang, and C. Miao, "Compact UWB bandpass filter with a notched band using radial stub loaded resonator," *IEEE Microwave Wireless Comp. Lett*., vol. 22, no. 7, pp. 351-353, 2012.

[15] M. J. Gao, L. S. Wu, and J. F. Mao, "Compact notched ultra-wideband bandpass filter with improved out-of-band performance using quasi electromagnetic bandgap structure," *Progress in Electromagnetics Research*, vol. 125, no. 17, pp. 137-150, 2012.

[16] F. Wei, W. T. Li, X. W. Shi, and Q. L. Huang, "Compact UWB bandpass filter with triple-notched bands using triple-mode stepped impedance resonator," *IEEE Microwave Wireless Comp. Lett.*, vol. 22, no. 10, pp. 512-514, 2012.

[17] F. Wei, Q. Y. Wu, X. W. Shi, and L. Chen, "Compact UWB bandpass filter with dual notched bands based on SCRLH resonator," *IEEE Microwave Wireless Comp. Lett*., vol. 21, no. 1, pp. 28-30, 2011.

[18] Y. Li, W. Li, C. Liu, and Q. Ye, "A compact UWB band-pass filter with ultra-narrow tri-notch-band characteristic," *Applied Computational Electromagnetics Society Journal*, vol. 29, no. 2, pp. 170-177, 2014.

[19] G. M. Yang, R. Jin, C. Vittoria, V. G. Harris, and N. X. Sun, "Small ultra-wideband (UWB) bandpass filter with notched band," *IEEE Microwave Wireless Comp. Lett.*, vol. 18, no. 3, pp. 176-178, 2008.

Ying Jiang Guo received the B.E. degree in Electronic Engineering from the Sichuan University (SCU), Chengdu, China in 2008, and received M.E. in Electromagnetic Field and Microwave Technology from the University of Electronic Science and Technology of China (UESTC), Chengdu, China in 2011, where he is currently working toward the Ph.D. degree in Electromagnetic Field and Microwave Technology. From 2011 to 2013, he was with the Chengdu Research Institute of Huawei Technology Ltd., where he was involved in the pre-research of ultra-wideband power amplifier, high frequency clock for AD and 5G communication prototype design. From 2013 to 2014, he was with the Sichuan Normal University, where he was a Lecturer. He has filed/granted a number of China patents in microwave circuit and internet of vehicle. His research interests include RF/microwave/mm-wave circuits design, antennas design, and monolithic-microwave integrated circuit applications.

Xiao Hong Tang was born in Chongqing, China, in 1962. He received the M.S. and Ph.D. degrees in Electromagnetism and Microwave Technology from the University of Electronic Science and Technology of China (UESTC), Chengdu, China, in 1983 and 1990, respectively. In 1990, he joined the School of Electronic Engineering, UESTC, as an Associate Professor, and became a Professor in 1998. He has authored or co-authored over 80 technical papers. His current research interests are microwave and millimeter-wave circuits and systems, microwave integrated circuits, and computational electromagnetism.

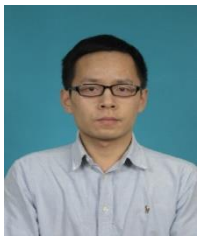

Kai Da Xu received the B.S. and Ph.D. degrees in Electromagnetic Field and Microwave Technology from University of Electronic Science and Technology of China (UESTC), Chengdu, China, in 2009 and 2015, respectively. He is now an Assistant Professor with Institute of Electromagnetics and Acoustics, and Department of Electronic Science, Xiamen University, Xiamen, China.

From September 2012 to August 2014, he was a Visiting Researcher in the Department of Electrical and Computer Engineering, Duke University, Durham, NC, under the financial support from the China Scholarship Council (CSC). He received the UESTC Outstanding Graduate Awards in 2009 and 2015. He was the recipient of National Graduate Student Scholarship in 2012, 2013, and 2014 from Ministry of Education, China. He has authored and co-authored over 40 papers in peer-reviewed journals and conference proceedings. Since 2014, he has served as a Reviewer for some journals including IEEE Transactions on Microwave Theory and Techniques, IEEE Transactions on Electron Devices, IEEE Transactions on Computer-Aided Design of Integrated Circuits and Systems, IEEE Transactions on Applied Superconductivity, International Journal of RF and Microwave Computer-Aided Engineering, ACES Journal, PIER, JEMWA and Journal of Engineering. His research interests include RF/microwave and mm-wave circuits, antennas, and nanoscale memristors.